Available online at www.sciencedirect.com
SCIENCE DIRECT®
International Journal of Mass Spectrometry 227 (2003) 111–120
International Journal of Mass Spectrometry
www.elsevier.com/locate/ijms

Binding of metalloporphyrins to model nitrogen bases: collision-induced dissociation and ion–molecule reaction studies

Lisa A. Hayes, Angelina M. Chappell, Emily E. Jellen, Victor Ryzhov*

Department of Chemistry and Biochemistry, Northern Illinois University, DeKalb, IL 60115, USA

Received 14 October 2002; accepted 19 November 2002

Dedicated to Prof. Robert C. Dunbar on the occasion of his 60th birthday and in deep appreciation of his invaluable mentoring and friendship.

Abstract

Binding of several volatile nitrogen bases to four metalloporphyrin cations was studied by collision-induced dissociation (CID) as well as ion–molecule reactions in a quadrupole ion trap mass spectrometer. Relative binding energy order was obtained from the CID data by comparing the stability of metalloporphyrin–amine complexes while accounting for the effects of the complex size. The efficiencies of ion–molecule association reactions were also used to compare binding in these systems. The results from these two approaches agree with each other. There appears to be no direct correlation between the proton affinity of model bases with their metalloporphyrin affinity. This discrepancy is rationalized in terms of steric hindrance and dipole moment effects.

Keywords: Collision-induced dissociation; Ion–molecule reactions; Metalloporphyrins; Metalloporphyrin–ligand binding

1. Introduction

Metalloporphyrin–ligand binding represents an important segment of biologically important non-covalent interactions [1]. The central metal atoms of metalloporphyrins are involved in a number of biologically important ligand binding processes [2]. Among these is reversible binding to protein basic sites, most often the nitrogen of a His side chain [1]. Such non-covalent complexes can be rather strong, as in myoglobin and cytochrome *a*, where the heme moiety is connected to the protein solely through the heme iron-histidine nitrogen coordinative bond as shown in Fig. 1. Metalloporphyrins are also believed to be involved in the cellular delivery of oligonucleotides [3]. There are numerous studies of the interaction of heme or other metalloporphyrins with various ligands [4,5] in different solvents resulting in the derivation of binding constants. However, thermochemical information about metal–ligand bonding in the absence of solvent effects is not abundant and still remains a challenge to gather.

Mass spectrometry has been shown to be a powerful tool for characterization of non-covalent complexes [6] including metalloporphyrin–ligand binding in model systems [7] and heme proteins [8]. The

* Corresponding author. Tel.: +1-815-753-6955; fax: +1-815-753-4802.
E-mail address: ryzhov@niu.edu (V. Ryzhov).

1387-3806/03/$ – see front matter © 2003 Elsevier Science B.V. All rights reserved.
doi:10.1016/S1387-3806(03)00045-9

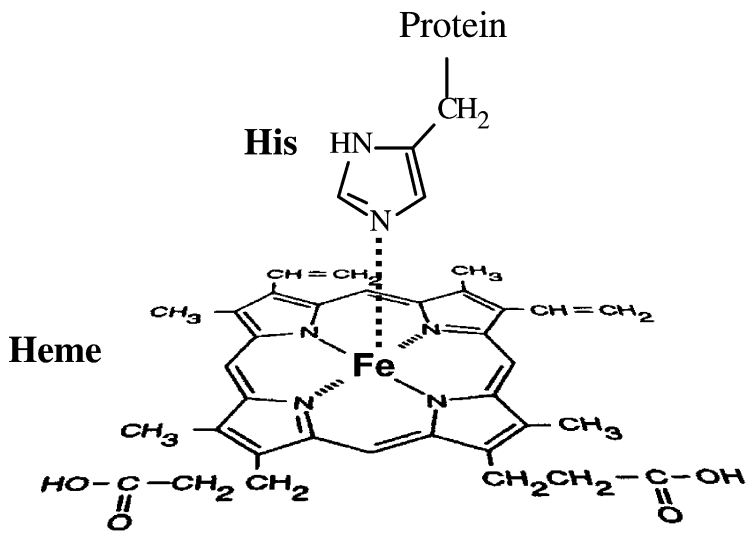

Fig. 1. Metal–ligand non-covalent binding in heme proteins.

stability of heme proteins was probed by collision-induced dissociation (CID) [9] and blackbody infrared dissociation (BIRD) [10] developed in part by Dunbar and co-workers [11–13]. The use of mass spectrometry to probe the strength of metalloporphyrin–ligand interactions has been relatively rare. Ridge and co-workers published a report on nitric oxide affinities of several iron porphyrins [14]. They used the aforementioned BIRD, associative equilibrium in FT-ICR conditions, and the radiative association kinetics (RAK) method developed by Dunbar [15,16].

Although these techniques provide ways to get accurate thermochemical information, they require the use of high-cost FT-ICR equipment. CID, which can be carried out on substantially less expensive quadrupole ion-trap mass spectrometers, could sometimes offer a worthwhile alternative to these FT-MS techniques. The utility of CID data to estimate bonding parameters was recognized by Hart and McLuckey [17] and Colorado and Brodbelt [18] through a variable energy CID technique. Similar to the threshold CID experiments [19,20] normally carried out on guided ion beam mass spectrometers, variable energy CID probes the kinetic stability of ions. CID in quadrupole ion traps has been widely used for relative binding energy comparisons between systems of similar size [21,22]. A qualitative correlation between CID stability and critical energy has been established [17,21,22].

In our recent work, we proposed a way to compare CID stability data for metalloporphyrin–ligand complexes of different size [23]. Here we continue to evaluate this approach for obtaining the relative binding energy of several model nitrogen bases to metalloporphyrin cations. We have picked several amines whose proton affinities fall between those of His and peptide N-terminus, the two anchors whose CID stability/size-dependence is known from our previous study [23].

Another route to binding energy information that we are exploring here is ion–molecule association reactions between metalloporphyrin cations and volatile nitrogen bases. The relatively high pressures of the quadrupole ion trap (compared to FT-MS) environment do not permit the use of the RAK method for accurate binding energy predictions. However, we would like to test the usefulness of comparisons of association rates for determining the relative order of binding energies. Also, if associative equilibrium conditions are achieved [24], the binding thermodynamics can be easily estimated, similar to FT-MS experiments [14,25].

2. Experimental

2.1. Reagents

Hemin (heme chloride), 5,10,15,20-tetraphenyl-21*H*,23*H*-porphine iron(III) (TPP-Fe) chloride, 5,10,15,20-tetraphenyl-21*H*,23*H*-porphine manganese(III) (TPP-Mn) chloride, 5,10,15,20-tetraphenyl-21*H*,23*H*-porphine cobalt(II) (TPP-Co), pyridine (Py), piperidine (Pipe), diisopropylamine (DIA), triethylamine (TEN), 4-picoline (MePy), 4-methoxypyridine (MeO-Py), 3-fluoropyridine (F-Py), diazabicyclo [2,2,2]octane (DBO), and quinuclidine (1-azabicyclo[2,2,2] nonane, Qui) were purchased from Sigma-Aldrich Chemical Company. Acetonitrile and acetic acid were purchased from Fisher Scientific. All chemicals were used without further purification.

Complexes of metalloporphyrins with amines were formed by mixing 20–100 μM solutions of a metalloporphyrin and an amine in water:acetonitrile (1:1, v/v).

2.2. Mass spectrometry

Experiments were done on a Bruker Esquire 3000 quadrupole ion trap mass spectrometer (Bruker Daltonics, Billerica, MA) equipped with an ESI source. Solutions containing 10–50 μM of a complex of interest were directly infused by a syringe pump at a flow rate of 4 μL min^{-1}. ESI source conditions were as follows: Nebulizer gas, 15 psi; dry gas, 5 psi; capillary temperature, 200 °C. Capillary exit and skimmer voltages were optimized to maximize the yield of ions corresponding to the *m*/*z* of interest. These ions were isolated in the ion trap and subjected to CID.

2.2.1. CID experiments

Variable energy CID experiments were done by ramping the resonance excitation voltage from 0 V to the value corresponding to the total dissociation of the complex (this value varied between 0.25 and 0.40 V, depending on the complex). The fragmentation delay was set to 0 ms, and the fragmentation width was 10 *m*/*z*. $E_{1/2}$ voltages were taken as the resonance excitation voltage values at which the intensity of the porphyrin–peptide complex and the porphyrin ions were equal. The fragmentation time was kept constant at 40 ms. Each data point was an average of three to four measurements.

2.2.2. Ion–molecule reactions

Metalloporphyrin cations were formed by ESI from 10 to 50 μM solutions of the respective chlorides, except for TPP-Co^+ which was formed by the one-electron oxidation of 5,10,15,20-tetraphenyl-21*H*,23*H*-porphine cobalt(II) during the ionization process. The ions of interest were isolated and stored in the ion trap for variable periods of time ranging from 50 ms to 5 s, during which reactions between the metalloporphyrin cation and a base were allowed to proceed. Volatile amines were introduced into the ion trap using the method of Gronert [26,27], where liquid amine is mixed into the He delivery line at a rate controlled by a syringe pump (Fisher). The flow of He was measured by a gas flow meter (Kurt-Lesker). From the He/amine flow ratio, an amine pressure in the trap can be estimated. Pressure of the amine ranged from 1×10^{-7} to 5×10^{-6} Torr. The uncertainty in pressure was about 30%. Metalloporphyrin–ligand complexes formed in the gas-phase were also subjected to variable energy CID according to the protocol described above.

2.3. Dipole moments, polarizabilities, and collision rate constants

Dipole moment values were obtained from the CRC Handbook [28] or estimated by AM1 semiempirical calculations using the HyperChem 6.03 program suite and scaled to match the experimental values where available. Molecular polarizabilities of model bases were calculated by the approach of Miller and Savchik [29]. Ion–molecule collisional rate constants, k_f, were calculated using the Langevin equation and then dipole-corrected as described by Su and Chesnavich [30].

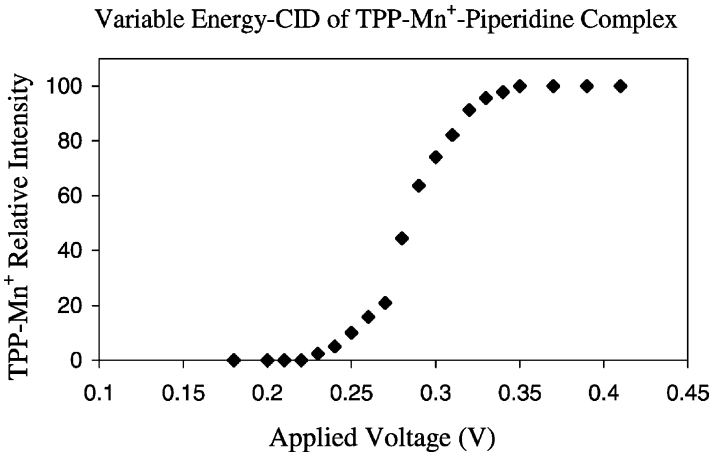

Fig. 2. Variable energy CID curve of heme–pyridine complex.

3. Results

3.1. Collision-induced dissociation data

Every metalloporphyrin ion–ligand complex yielded a simple CID spectrum resulting in the production of the metalloporphyrin cation as a unique product. We could not find satisfactory experimental conditions to form complexes of TPP-Co with DIA and TEA. A typical variable energy CID curve is shown in Fig. 2. From curves like this, $E_{1/2}$ values were taken as the voltages required to produce equal

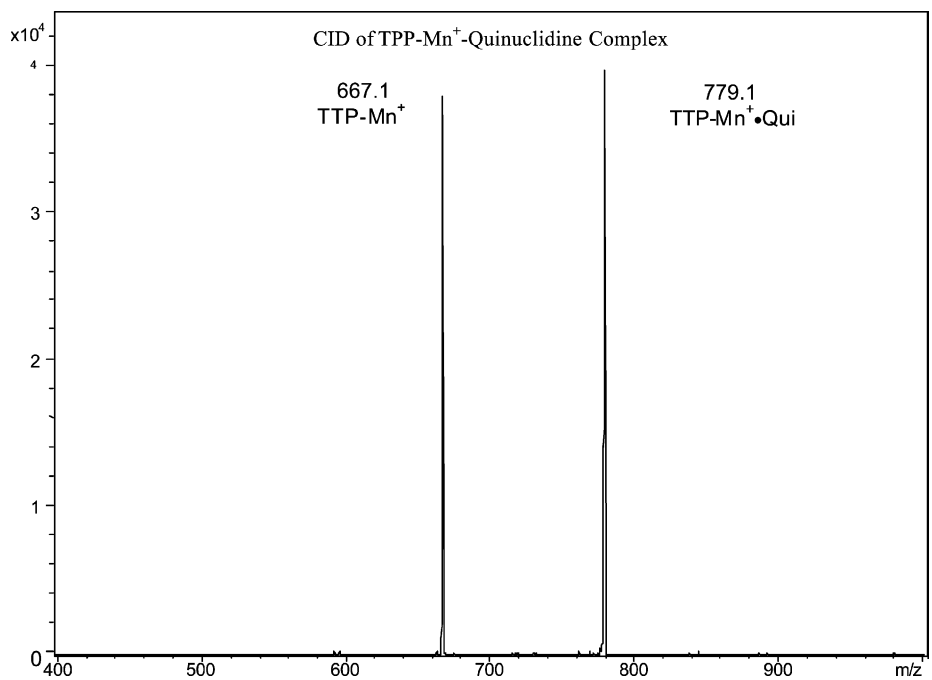

Fig. 3. CID mass spectrum of a TPP-Mn^{+}–quinuclidine complex.

Table 1
Number of degrees of freedom (DF) and experimental $E_{1/2}$ values (Volts) of nitrogen base–metalloporphyrin complexes and polarizability (α) and dipole moment (μ) values of nitrogen bases

Base	α (Å^3)	(μ) D	TPP-M$^+$ base				Heme$^+$ base	
			DF	$E_{1/2}$ (Co)	$E_{1/2}$ (Fe)	$E_{1/2}$ (Mn)	DF	$E_{1/2}$
3-Fluoropyridine	9.16	2.09	258	0.31	0.315	0.32	252	0.30
Pyridine	9.18	2.19	258	0.34	0.35	0.35	252	0.325
4-Picoline	11.32	2.70	267	0.37	0.37	0.37	261	0.35
4-Methoxypyridine	11.98	2.95	270	0.38	0.39	0.38	264	0.36
Piperidine	11.36	0.82	276	0.36	0.39	0.39	270	0.37
Diisopropylamine	13.34	0.90	291	0.40	0.40	–	285	0.38
Triethylamine	13.38	0.66	291	0.41	0.40	–	285	0.38
Diazabicyclooctane	13.38	0	285	0.42	0.40	0.395	279	0.38
Quinuclidine	13.70	1.37	288	0.425	0.42	0.41	282	0.40

intensities of the initial metalloporphyrin ion–ligand complex and the resulting metalloporphyrin cation. Fig. 3 shows an example of a CID mass spectrum of TPP-Mn$^+$–quinuclidine complex taken at an $E_{1/2}$ voltage value of 0.4 V. $E_{1/2}$ values for complexes of the four metalloporphyrins and nine ligands are given in Table 1.

3.2. Ion–molecule reactions

Electrospray-generated metalloporphyrin cations underwent association reactions with model nitrogen bases by sequentially attaching two molecules of the base. An illustrative mass spectrum for the association of heme cation and piperidine is shown in Fig. 4. The

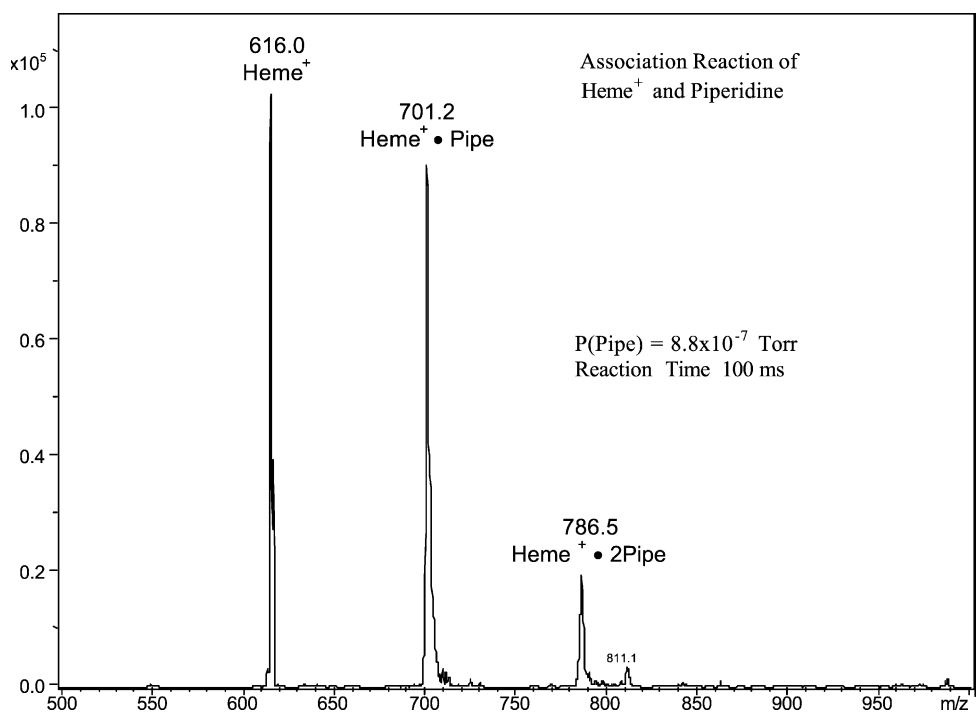

Fig. 4. A mass spectrum of a heme–piperidine association reaction taken after 100 ms reaction time and piperidine pressure of 8.8×10^{-7} Torr.

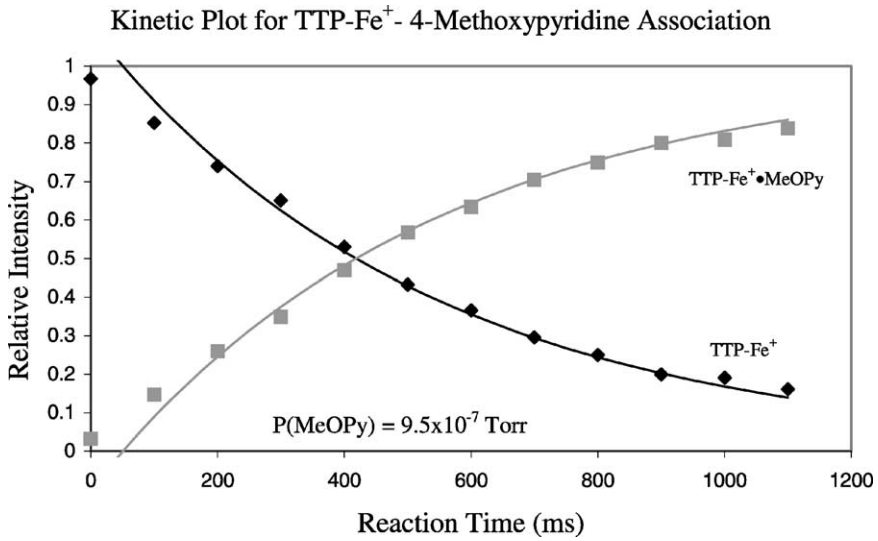

Fig. 5. A kinetic plot for the association reaction of TPP-Mn^+ with 4-methoxypyridine.

spectrum displays major peaks at m/z 616 (heme$^+$), 701 (heme$^+$·piperidine), and 786 (heme$^+$·2 piperidine). Kinetic analysis was done for the attachment of the first ligand only. A typical kinetic plot is given in Fig. 5. Data were fitted to pseudo-first-order kinetics. Small induction periods (50 ms or smaller, depending on the pressure) were observed corresponding to the time needed to fully thermalize the ions. Data points within these time periods were not included in the fit procedures. For each association reaction several pressures ranging from 1×10^{-7} to 5×10^{-6} Torr were utilized to ensure no significant pressure-dependence of the rate constants. Average values of the rate constants were used. No useful kinetics were obtained in reactions of TPP-Mn and TPP-Co with DIA as well as TPP-Mn with TEA due to interferences. The reaction of TPP-Fe with TEA reached equilibrium under experimental conditions. The bimolecular association rate constants k_2 (in 10^{-10} cm^3 s^{-1}) and efficiencies (k_2/k_f, %) are given in Table 2.

Table 2
Collision (k_f) and experimental (k_2) association rate constants (10^{-10} cm^3 s^{-1}) and efficiencies ($\Phi = k_2/k_f$, %) for reactions of metalloporphyrin cations with neutral bases

Base	Heme			TPP						
	k_f	k_2	Φ	k_f[a]	k_2 (Mn)	Φ (Mn)	k_2 (Fe)	Φ (Fe)	k_2 (Co)	Φ (Co)
3-Fluoropyridine	13.6	2.3	17	13.5	1.9	14	1.4	10	3.2	23
Pyridine	15.4	2.6	13	15.3	2.1	14	1.5	10	3.3	22
4-Picoline	17.0	2.8	16	16.9	2.5	15	1.9	11	4.0	24
4-Methoxypyridine	17.0	2.9	17	16.9	2.6	15	2.0	12	4.5	27
Piperidine	10.5	2.4	23	10.4	2.0	19	1.5	14	1.4	13
Diisopropylamine	10.5	1.4	13	10.5	–	–	1.1	10	–	–
Triethylamine	10.1	1.3	13	10.0	–	–	Eq.[b]	–	0.6	6

[a] The same collisional rate constants k_f were used for TPP-Mn, TPP-Fe, and TPP-Co.
[b] Eq.: equilibrium was observed.

4. Discussion

4.1. CID data correction for size effects

4.1.1. Heme–amine complexes

Variable energy CID offers a straightforward approach for binding energy comparisons between systems of similar size and structure [21]. When there is a size (or the number of degrees of freedom) variation between the systems under comparison, size effects have to be known. Recently [23], we have determined effects of size on stability for metalloporphyrin complexes where the metal is bound to the side chain of His or the peptide N-terminus. Here these stability/size-dependence plots are used for comparisons of model nitrogen base binding. Fig. 6 shows such comparison for heme complexes. The $E_{1/2}$ values of heme–nitrogen base complexes are plotted against the number of degrees of freedom of the complex. The upper line represents a linear fit for the data for heme–His-containing peptide complexes, and the lower line is the fit for the heme–peptide N-terminus binding data [23]. While there is an experimental uncertainty associated with these linear fits, the slopes for heme, TPP-Fe, and TPP-Mn were found to be nearly identical [23]. This is in agreement with the findings of Vachet et al. [31] who showed that a Rice–Rampsberger–Kassel model predicts that rather substantial differences (in the order of 1 eV) in critical energies between systems are needed to obtain a noticeable slope change. In our case, the differences between binding energies are much smaller.

One can see that the CID stability of all heme-model nitrogen base complexes under study falls between those of heme–His and heme-N-terminus. This is not unexpected, since proton affinities of these bases (see Table 1) mostly lie between those of His (232 kcal mol^{-1}) and the peptide N-terminus (212–217 kcal mol^{-1}) [32]. The relative heme affinity order can be constructed by evaluating the y-difference between the His and model base data in Fig. 6. Such inspection yields the following heme binding energy order:

$$\text{N-terminus} < \text{TEA} \approx \text{DIA} < \text{F-Py} < \text{DBO} < \text{Pipe} \approx \text{Qui} < \text{Py} \approx \text{MePy} \approx \text{MeOPy} < \text{His side chain}$$

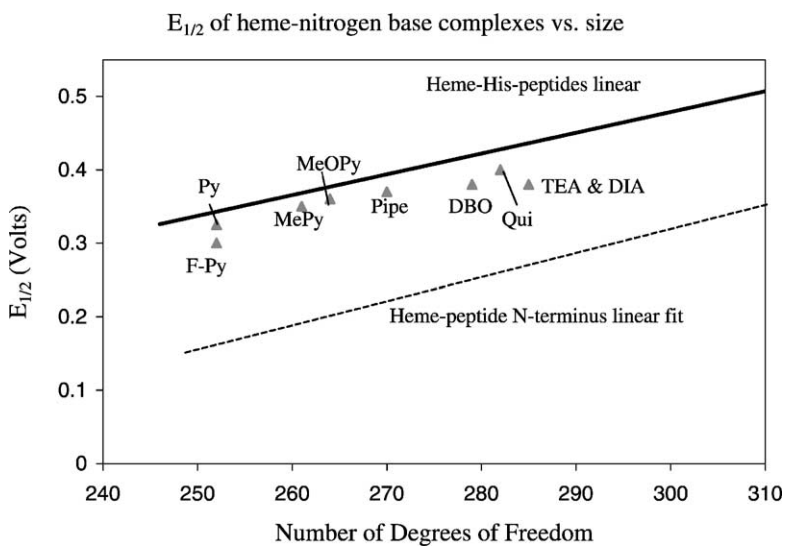

Fig. 6. Dependence of the $E_{1/2}$ values of complexes of heme and model amines on the complex size. Triangles represent experimental data from Table 1. Lines are best linear fits for complexes of heme with His-containing peptides (upper line) and with peptide N-termini (lower line) taken from [23].

This order does not correlate well with the proton affinities of these bases. Polarizability was shown to be a major factor in the binding of bare metal cations to substituted pyridines [33,34]. However, polarizability effects should be included in the proton affinity values. To better understand the differences between the proton affinity (formation of a covalent nitrogen–hydrogen bond) and heme affinity (formation of a coordinative iron–nitrogen bond), one should also take into account the dipole moment values (see Table 1) of the bases since ion–permanent dipole interaction will also have a substantial contribution to the bonding [33,34]. DBO has no dipole moment, and TEA and DIA have smaller dipole moments than other bases. In addition, steric hindrance could be a factor in TEA and DIA binding. It seems that the combination of a relatively high dipole moment and a favorable binding geometry puts pyridine, picoline, and methoxypyridine on top of the heme binding order.

4.1.2. Tetraphenylmetalloporphyrin–amine complexes

Analysis of the three tetraphenylmetalloporphyrin (TPP-Mn, Fe, and Co) complexes performed similarly to Fig. 6 (data not shown) showed relative binding energy trends identical to the heme–nitrogen base results. The similarity between heme and TPP-ligand binding, and some other iron porphyrin-ligand binding was shown in the literature [14]. There was very little difference in nitrogen base binding between iron, cobalt, and manganese TPPs. This correlates very well with X-ray structures of TPP–metal complexes with various ligands where there is less than 1% difference in metal–ligand distances between Mn, Fe, and Co [35].

4.2. Comparing CID stability of complexes formed in solution and in the gas-phase

To test the similarity of structure of ion–neutral complexes formed in solution as well as in the gas-phase, we compared their stability under CID conditions. The gas-phase experiments consisted of forming a metalloporphyrin cation by ESI, isolating it in the ion trap, letting it react with a base of interest, isolating the 1:1 complex, and, finally, subjecting the complex to a variable energy CID procedure. For all four porphyrins under study, complexes with Py, Pipe, DIA and TEA formed either in the gas-phase or in solution had the same $E_{1/2}$ values (± 0.005 V) independent of their origin, or way of formation. While this does not fully prove that metalloporphyrin–ligand complexes formed by ESI from solution and those formed in the gas-phase have exactly the same structure, this gives us some confidence to use gas-phase studies in these systems to obtain thermochemical information relevant for solution chemistry.

4.3. Ion–molecule association results

An ion–neutral association reaction can be analyzed in terms of the detailed mechanism in Eq. (1)

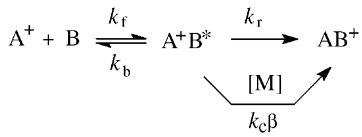

(1)

where k_f is the bimolecular rate constant for collisional complex formation (orbiting rate), k_b the unimolecular redissociation rate constant, k_r the unimolecular rate constant for IR photon emission from the energized complex, and $k_c\beta$ is the bimolecular rate constant for collisional stabilization of A^+B^* by collision with neutral M (He in ion traps), and A^+B^* is the metastable collision complex.

This mechanism gives the following expression for the overall bimolecular rate constant k_2:

$$k_2 = \frac{k_f k_r}{k_b + k_r} + \frac{k_f k_c \beta k_b [M]}{(k_b + k_r)^2} \quad (2)$$

In ion trap conditions, where He pressure is on the order of millitorrs, three-body collisional stabilization of the complex is predominant and the first term can be ignored. The kinetics will simplify to give the following expression for the association efficiency:

$$\Phi = \frac{k_2}{k_f} = \frac{k_c \beta k_b [M]}{(k_b + k_r)^2} \quad (3)$$

In this equation the He collisional efficiency β is not known, but it should be nearly constant for similar metalloporphyrin ion–neutral ligand complexes provided there is no great variation in the ligand size. The k_r is normally much smaller than k_b which, in turn, has a direct connection to binding energy and the size of the system [16]. Thus, if the ligand size is similar, the association efficiency should reflect the relative binding energy order.

Table 2 lists the association rate constants and efficiencies obtained for the reactions between four metalloporphyrin cations and volatile nitrogen bases. For most systems, the efficiencies are in the range of 10–25%. The large uncertainty in pressure measurements present in these experiments does not allow us to make useful comparisons in these systems, similar to low-pressure radiative association limitations [16]. It seems that TEA and DIA do display one of the lowest efficiencies, in agreement with the CID data. One interesting case is the association of TPP-Fe cation with TEA, where equilibrium conditions were established. This supports the finding that TEA has one of the lowest affinities towards metalloporphyrins among the nitrogen bases under consideration since for all other systems under experimental conditions the equilibrium lies considerably towards the association side. The equilibrium data will permit the calculation of ΔG in this system, and a way to calculate the binding energy, ΔH, through ΔS modeling in a future work. The differences in the association efficiencies between heme, TPP-Fe, and TPP-Mn are not significant. This is supported by the work of Ridge and co-workers who measured similar NO affinities for heme and TPP-Fe [14]. TPP-Co displayed slightly higher association efficiencies for most nitrogen bases compared to other metalloporphyrins. As an outlook for the future use of this approach, it seems that larger differences in ligand binding energies are needed for successful discrimination of association efficiency data. It is also desirable to work in the regime of substantially lower association efficiencies where pressure uncertainties will not play such a large role.

5. Conclusions

Relative binding energy order was obtained for heme and three tetraphenylmetalloporphyrin cation complexes with nine model nitrogen bases from variable energy CID experiments. The data were interpreted by accounting for the size effects using the metalloporphyrin–peptide complex "stability versus size" diagrams. Pyridyl ligands displayed the highest metalloporphyrin affinity, which does not correlate well with their relative proton affinity. This discrepancy is rationalized in terms of relatively high dipole moments of substituted pyridines as well as the absence of steric hindrance in their binding. Not much variation was found between tetraphenylporphyrin-iron, manganese, or cobalt binding. Metalloporphyrin cation–ligand ion–molecule association reactions in an ion trap were also tested as a way to probe the binding energy order of different nitrogen ligands. The large pressure uncertainty in these experiments rendered them inconclusive as the association efficiencies were quite similar in all systems. The efficiencies were on the low side for diisopropylamine and triethylamine, in agreement with the CID data. Moreover, equilibrium was reached in the reaction of TPP-Fe^+ with triethylamine, which provides a direct route to thermochemistry of this system.

Acknowledgements

This work was supported in part by the American Society for Mass Spectrometry Research Award. Generous support from the Department of Chemistry and Biochemistry, the Graduate School, and the College of Liberal Arts and Sciences of Northern Illinois University is gratefully acknowledged. The authors thank Mr. Marvin Banal for his help with dipole moment calculations.

References

[1] E. Antonini, M. Brunori, Hemoglobin and Myoglobin in their Reactions with Ligands, North-Holland, Amsterdam, 1971.

[2] K.M.E. Smith, Porphyrins and Metalloporphyrins, Elsevier, Amsterdam, 1975.
[3] S.M. Flynn, S.T. George, L. White, W. Devonish, G.B. Takle, Biotechniques 26 (1999) 736–742, 744, 746.
[4] R.F. Pasternack, B.S. Gillies, J.R. Stahlbush, J. Am. Chem. Soc. 100 (1978) 2613.
[5] F.A. Walker, M. Benson, J. Am. Chem. Soc. 102 (1980) 5530.
[6] J.A. Loo, Mass Spectrom. Rev. 16 (1997) 1.
[7] H.L. Chen, T.E. Hagan, S.E. Groh, D.P. Ridge, Org. Mass Spectrom. 26 (1991) 173.
[8] R.K. Upmacis, D.P. Hajjar, B.T. Chait, U.A. Mirza, J. Am. Chem. Soc. 119 (1997) 10424.
[9] Y.L. Chen, J.M. Campbell, B.A. Collins, L. Konermann, D.J. Douglas, Rapid Commun. Mass Spectrom. 12 (1998) 1003.
[10] D.S. Gross, Y.X. Zhao, E.R. Williams, J. Am. Soc. Mass Spectrom. 8 (1997) 519.
[11] R.C. Dunbar, T.B. McMahon, D. Tholmann, D.S. Tonner, D.R. Salahub, D.Q. Wei, J. Am. Chem. Soc. 117 (1995) 12819.
[12] R.C. Dunbar, J. Phys. Chem. 98 (1994) 8705.
[13] R.C. Dunbar, T.B. McMahon, Science 279 (1998) 194.
[14] O. Chen, S. Groh, D.P. Ridge, Orlando, FL, 1998, p. 862.
[15] R.C. Dunbar, Int. J. Mass Spectrom. Ion Process. 100 (1990) 423.
[16] R.C. Dunbar, Int. J. Mass Spectrom. Ion Process. 160 (1997) 1.
[17] K.J. Hart, S.A. McLuckey, J. Am. Soc. Mass Spectrom. 5 (1994) 250.
[18] A. Colorado, J. Brodbelt, J. Am. Soc. Mass Spectrom. 7 (1996) 1116.
[19] M.T. Rodgers, P.B. Armentrout, Mass Spectrom. Rev. 19 (2000) 215.
[20] P.B. Armentrout, J. Am. Soc. Mass Spectrom. 13 (2002) 419.
[21] M.L. Reyzer, J.S. Brodbelt, S.M. Kerwin, D. Kumar, Nucleic Acids Res. 29 (2001) E103.
[22] M. Satterfield, J.S. Brodbelt, Inorg. Chem. 40 (2001) 5393.
[23] E.E. Jellen, A.M. Chappell, V. Ryzhov, Rapid Commun. Mass Spectrom. 16 (2002) 1799.
[24] M.Y. Combariza, R.W. Vachet, J. Am. Soc. Mass Spectrom. 13 (2002) 813.
[25] V. Ryzhov, R.C. Dunbar, J. Am. Soc. Mass Spectrom. 10 (1999) 862.
[26] S. Gronert, J. Am. Soc. Mass Spectrom. 9 (1998) 845.
[27] S. Gronert, J. Mass Spectrom. 34 (1999) 787.
[28] D.R. Lide (Ed.), CRC Handbook of Chemistry and Physics, 76 ed., CRC Press, Boca Raton, 1995/1996.
[29] K.J. Miller, J.A. Savchik, J. Am. Chem. Soc. 101 (1979) 7206.
[30] T. Su, W.J. Chesnavich, J. Chem. Phys. 76 (1981) 5183.
[31] R.W. Vachet, A.D. Winders, G.L. Glish, Anal. Chem. 68 (1996) 522.
[32] S.G. Lias, J.F. Liebman, R.D. Levin, J. Phys. Chem. Ref. Data 13 (1984) 695.
[33] M.T. Rodgers, J. Phys. Chem. A 105 (2001) 8145.
[34] M.T. Rodgers, J. Phys. Chem. A 105 (2001) 2374.
[35] W.R. Scheidt, Acc. Chem. Res. 10 (1977) 339.